Journal of Applied Mechanics and Technical Physics, Vol. 37, No. 3, 1996

GAS-DENSITY-DISTRIBUTION MEASUREMENT USING AN ELECTRON BEAM AND COMPUTERIZED TOMOGRAPHY TECHNIQUES

V. G. Prikhod'ko, A. I. Sedel'nikov,* S. N. Ul'yankin, and V. N. Yarygin

UDC 533.6.07

Introduction. When studying complex gas-dynamic objects, it is necessary to have an idea of the flow structure as a whole. To this end, various methods are employed: shadowgraphy, speckle photography, interferometry (including holographic), and visualization using gas discharge and an electron beam [1–4]. Recently, many papers have appeared in which tomographic methods are offered for analysis of flow geometry and characteristics [5–7].

Optical methods are insufficiently sensitive for studying rarefied gas flows. The electron-beam method is considered more suitable. It is a rather difficult task to determine the entire flow structure using an electron beam. It is necessary to photograph the optical radiation formed and to perform densitometric treatment of negatives taking into account the photomaterial properties. If the gas particle density is $n < 3 \cdot 10^{13}$ cm^{-3}, the electron-excited radiation becomes weak even for luminous gases (nitrogen and helium), and density measurements using this method become impossible.

At the same time, there is a method for measuring density by attenuation of an electron beam passing through the volume examined that retains its sensitivity in a more rarefied gas. This is an integral method and it is necessary to apply an Abel transform to reconstruct the density distribution, which is possible only in axisymmetric flows. If density is reconstructed by reconstructive tomography methods, a flow structure with an arbitrary configuration can be determined.

This paper proposes a method of density field determination in three-dimensional rarefied gas flows that is based on the results of measurement of electron beam attenuation as a function of beam position and orientation relative to the flow. Spatial density distribution is reconstructed by one of the reconstructive tomography methods for a plane beam, namely, the filtered back projection algorithm (in particular, its version with a fast Fourier transform). As an example, results are used that show the flow structure in a region of the interaction of two jets flowing from identically directed nozzles.

Experimental Setup. Test experiments were carried out using the low-density gas-dynamic setup shown schematically in Fig. 1. The gas flow source consisted of two nozzles with the same orientation with a stagnation chamber in common. Conical convergent nozzles with a 2-mm throat diameter were used. The distance between the nozzle centers was 51.5 mm. The source was located on a three-component positioning mechanism 7, which was used to move the object relative to the electron beam along (X axis) and across (Y axis) the flow and to turn it through an angle θ about the axis passing halfway between the nozzles parallel to the X axis. A three-electrode electron gun 4 generated a narrow electron beam with a diameter of 1 mm, an energy of 15 kV, and a current of up to 10 mA. Prior to the experiments, the test chamber 1 was evacuated to a pressure of 0.01 Pa, at which electrons did not scatter when crossing the chamber and the beam's cross-sectional dimensions remained constant. By means of deflection coils the electron beam was directed to an electron collector 6, which was a copper radiation-cooled Faraday cylinder in front of which

*Deceased.

Institute of Thermophysics, Siberian Division, Russian Academy of Sciences, Novosibirsk 630090.
Translated from Prikladnaya Mekhanika i Tekhnicheskaya Fizika, Vol. 37, No. 3, pp. 186–191, May–June, 1996. Original article submitted February 7, 1995; revision submitted March 24, 1995.

 0021-8944/96/3703-0454 $15.00

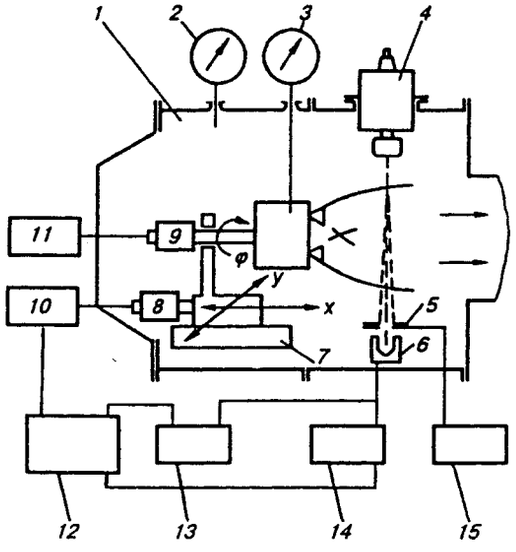

Fig. 1

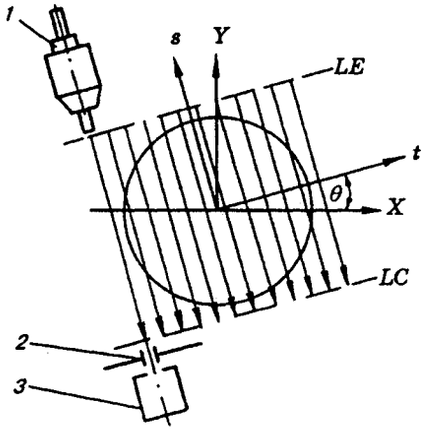

Fig. 2

a diaphragm 5 was placed to restrict the beam aperture. The diaphragm diameter was 2 mm; the distance between the diaphragm and electron gun outlet was 500 mm. A small (10–20 V) negative potential from a power supply 15 was fed to the diaphragm to decrease the influence of secondary electrons produced by inelastic collisions of primary beam electrons with gas molecules.

With gas flow, some of the beam's electrons, being scattering by gas molecules, were deflected from the initial direction and, thus, missed the diaphragm aperture. An attenuated electron beam that passed through the diaphragm was measured by a milliammeter 14 connected into the collector circuit. The signal was recorded by a data-acquisition system 12 using an SM-1420 computer and was sent to a plotter 13.

The following parameters were measured: the stagnation pressure (by a standard vacuum gauge 3), the test-chamber pressure (by a thermocouple vacuum gauge 2), and the emission i_e and collector i_c currents. Values of the coordinates x and y and the rotation angle θ were measured using BS-155 synchro transmitters (8 and 9) and F-5095 display units (10 and 11) and were recorded by the computer. At a fixed distance from the nozzles, $x_s = 10$–60 mm, transverse profiles of the collector current $i_c = f_i(y)$ were recorded for a discrete set of values of the angle θ. For the test experiments, the domain was $y = \pm 70$ mm. The angle θ was varied from 0 to π; 20 profiles were recorded. After scaling, the profiles obtained were considered as a set of projections for the calculation algorithm for spatial density reconstruction.

Algorithm. We studied complex flow with density distribution $n = f(x, y)$ in a fixed Cartesian coordinate system X, Y. This measurement system is related to the moving Cartesian coordinates s, t through an angle θ relative to the X, Y system (Fig. 2). The moving system includes the electron beam with emitter 1 on line LE at the coordinate $t = t_e$ and the diaphragm 2 with electron collector 3 on line LC with coordinate $t = t_c$ ($t_c - t_e = \text{const}$). When the emitter moves along line LE, the collector is shifted along LC. The emitter current i_e is constant along LE and the collector current i_c depends on s and the angle θ [8]:

$$i_c(s, \theta) = i_e \exp\Big(-\mu \int_{t_e}^{t_c} f_\theta(s, t) dt \Big).$$

In this case, $f_\theta(s, t)$ is the gas particle density in the s and t coordinates; μ is the coefficient of electron-beam attenuation. The profiles $i_c(s, \theta)$ are recorded experimentally.

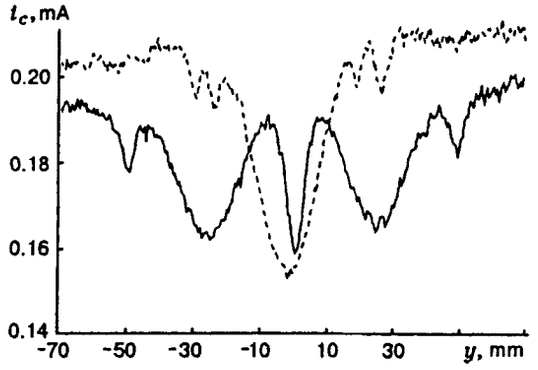

Fig. 3

The value $p(s,\theta) = -1/\mu \ln(i_c(s,\theta)/i_e)$ is the projection of the gas-density field onto LC determined as

$$p(s,\theta) = \int_{t_e}^{t_c} f_\theta(s,\theta)dt\,.$$

The function $f(x,y)$ can be reconstructed from a set of experimental data $p(s,\theta)$ by computerized tomography methods. In this case, the algorithm of filtration and back projection was used [9]. According to the theorem, on a central cross-section, we obtain

$$f(x,y) = \int_0^{\pi}\int_{-\infty}^{\infty} \hat{p}(R,\theta)\exp(i2\pi R(x\cos(\theta) + y\sin(\theta)))|R|\,dR\,d\theta\,,$$

where $\hat{p}(R,\theta)$ is the one-dimensional Fourier transform of the function $p(s,\theta)$. To construct the function $f_{\text{res}}(x,y)$, which is an approximation of the function $f(x,y)$ with a restricted spectrum width, it is necessary to introduce the window function $W(R)$ in the frequency domain. Hence,

$$f_{\text{res}}(x,y) = \int_0^{\pi}\int_{-1}^{+1} p(s,\theta)q(x\cos(\theta) + y\sin(\theta) - s)\,ds\,d\theta, \quad q(s) = \int_{-1/2\Delta s}^{+1/2\Delta s} |R|W(R)\exp(i2\pi Rs)\,dR.$$

These expressions are the basis of a method that is known as the convolution back-projection [9] or filtered back-projection [5] method. A fast Fourier transform algorithm was used to calculate the convolution of the functions p and q [10]. The following function was used as a filtering function:

$$q(s) = 2(k\pi)^2[\text{sinc}(2ks) - \text{sinc}^2(ks)].$$

Here $\text{sinc}(x) = \sin(\pi x)/\pi x$; $k = 2\pi^2\alpha/\Delta s$; Δs is the discretization interval of the variable s; and α is the chosen coefficient (with $\alpha = 1/4\pi$, function $q(s)$ transforms into the filtering function with a cosine window function $W(R)$ [11]).

Results. Measurement results demonstrating the possibilities of the above procedure are given in Figs. 3–5. The experimental conditions were the following: stagnation pressure $p_0 = 4\cdot10^4$ Pa; test-chamber pressure $p_c = 13$ Pa; stagnation temperature $T_0 = 300$ K. The Reynolds number calculated from the stagnation parameters and nozzle-throat diameter was $\text{Re}_0 = 1.8\cdot10^4$; the Reynolds number calculated from the jet length was $\text{Re}_L = \text{Re}_0/\sqrt{p_0/p_c} = 320$.

Figure 3 shows sample transverse profiles of the collector current i_c recorded in our experiments. The solid curve corresponds to $\theta = 0$, and the dotted curve, to $\theta = \pi/2$. Values of the current were recorded every 0.5 mm. The recording time of one profile is about 2 min; this time depends on the capabilities of the positioning mechanism and recording equipment. To check the efficiency of the technique, current profiles

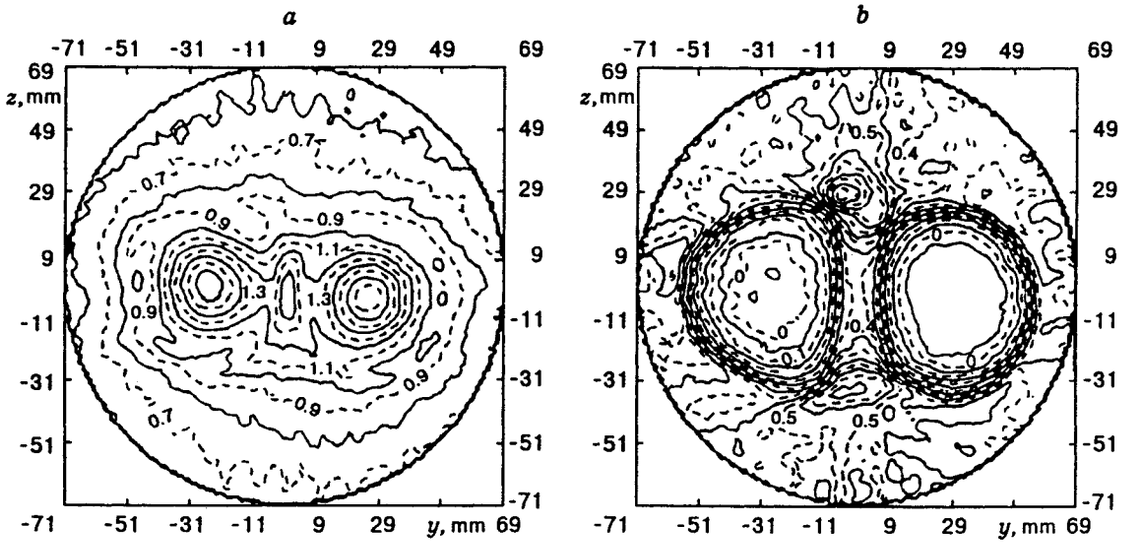

Fig. 4

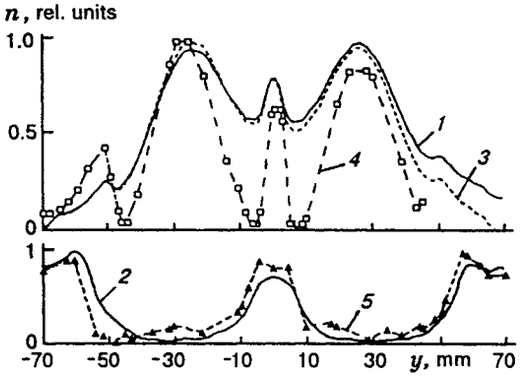

Fig. 5

were used in the calculations without any pretreatment (smoothing, taking into account emission current, etc.) and the cathode emission current in the electron gun was taken as the i_e value. The logarithms of the i_c/i_e values were interpolated on a uniform grid of s_i values to obtain a set of projections. These projections were used to reconstruct the image, i.e., the function $f_{\text{res}}(x, y)$ for values of x and y that lie inside a circle with a radius of 70 mm. At points s_i the convolutions of the functions $p(s, \theta)$ and $q(s)$ were determined and integrated over the angle θ. In the calculations we ignored beam-current attenuation and electron scattering by the background gas. The coefficient α was taken as unity.

Figure 4 shows equidensity curves at sections $x_s = 20$ and 50, respectively. Although the curves are not very smooth, because of noise and i_c measurement errors, they fairly adequately reproduce the flow structure. Figure 4a shows both a compressed region appearing at the center of the flow and its structure. The flow density decreases with increasing distance to the nozzle inlet and becomes lower than the gas density in the ambient medium (Fig. 4b). Also, two additional zones with increased density are observed in the region $y = 0$, $z = -31$ mm and $y = 0$, $z = 29$ mm.

Figure 5 presents reconstructed transverse profiles of normalized density $n(y) = (f_{\text{res}}(x_s, y) - f_{\min}(x_s))/(f_{\max}(x_s) - f_{\min}(x_s))$ along the line $z = 0$ passing through the centers of the nozzles. The subscripts min and max denote the minimum and maximum of the function $f_{\text{res}}(x_s, y)$. Curves 1 and 2 correspond to $x_s = 20$ and 50 mm. Note that on these profiles there is no high-frequency component of the measurement

noise, which was filtered-out for image reconstruction. A slow change in the beam current during recording (Fig. 3 shows that at the beginning and at the end of the profiles the values of the collector current are somewhat different) leads to a change in the density profiles, which can be taken into account by introducing appropriate corrections (curve 3).

Since the real density distribution in this flow is unknown, the reliability of the results can be estimated by comparing them with those obtained by other (conventional) methods. The dots and curves 4 and 5 in Fig. 5 are the results of local density measurements by recording the intensity of x-ray bremsstarhlung obtained as described in [12]. It can be seen that the behavior of the curves coincides qualitatively, but the contrast of the reconstructed image differs, however, from the measured one. The greatest deviation can reach 57% which is attributed to the unsuccessful choice of the function $q(s)$ and coefficient α.

The results obtained confirm the assumption that the above technique can be used to determine flow structure and the spatial distribution of rarefied gas density and show the characteristic features of the technique and aspects that require further analysis. To obtain quantitative results it is necessary to take into account the beam attenuation factor, the accurate value of the current i_c, and electron scattering by the molecules of the surrounding gas by choosing an optimal filtering function from a test object with a given density distribution.

REFERENCES

1. L. A. Vasil'yev, *Shadow Methods*, Nauka, Moscow (1968).
2. N. A. Fomin, "Application of speckle technique to diagnose gas-dynamic flows," Preprint No. 44, Institute of Heat and Mass Exchange, Acad. of Sci. of the BSSR, Minsk (1987).
3. Ch. West, *Holographic Interferometry* [Russian translation], Mir, Moscow (1982).
4. D. E. Rothe, "Flow visualization using a traversing electron beam," *AIAA J.*, **3**, No. 10 (1965).
5. V. V. Pikalov and N. G. Preobrazhenskii, *Computerized Tomography in Gas-Dynamics and Plasma Physics*, Nauka, Novosibirsk (1987).
6. A. I. Sedelnikov and A. I. Chernov, "Tomographic determination of the density field in the supersonic jet behind a slanted exit nozzle," *Izv. Sib. Otdel. Akad. Nauk SSSR, Ser. Tekh. Nauk*, **4**, 77–80 (1990).
7. L. C. Philippe, M. Y. Perrin, and M. Cohat, "Beam deflection tomography: application to two interacting parallel free-jets," in: *Rarefied Gas Dynamics*: Proc. 17th Int. Symp., Aachen, Germany, July 8–14, 1990, Weinheim (1991), pp. 1538–1544.
8. E. P. Busygin and G. K. Tumakaev, "Gas density measurement behind the shock wave in a shock tube using the electron-beam method," *Zh. Tekh. Fiz.*, **34**, No. 1 122–127 (1964).
9. R. M. Lewitt, "Reconstruction algorithm: transform methods," *Proc. IEEE*, **71**, 390–408 (1983).
10. E. O. Brigham and R. E. Morrow, "The fast Fourier transform," *IEEE Spectrum*, **4**, No. 12, 63–70 (1967).
11. G. Herman, *Image Reconstruction from Projections. The Fundamentals of Computerized Tomography*, Academic Press (1980).
12. N. G. Zharkova, L. I. Kuznetsov, A. K. Rebrov, and V. N. Yarygin, "Rarefied gas and plasma density measurement using an electron beam," *Teplofiz. Vys. Temp.*, **14**, No. 1, 17–20 (1976).